The Geological Society of America
Special Paper 516
2016

Morphometric analysis of cave patterns using fractal indices

Patricia N. Kambesis
Department of Geoscience, Mississippi State University, Mississippi State, Mississippi 39762, USA

Erik B. Larson
Department of Natural Sciences, Shawnee State University, Portsmouth, Ohio 45662, USA

John E. Mylroie
Department of Geoscience, Mississippi State University, Mississippi State, Mississippi 39762, USA

ABSTRACT

Cave type and morphology are controlled by hydrogeological and geological factors; therefore, by inverse analogy, cave type and morphology could be used to determine the hydrogeological and geological conditions under which the caves developed. Euclidian metrics have traditionally been used to quantify and compare cave morphologies, even though caves have irregular and complex shapes. Caves have been shown to possess characteristics that identify them as fractals within certain ranges, so the use of Euclidean-based metrics alone to define and characterize them may be a limitation in morphometric analyses. Other factors that limit full morphometric analyses of caves include focus on two-dimensional cave data, as these are typically what are available, and exploration bias, as cave exploration and documentation are limited to spaces that are humanly passable or of immediate interest to the explorer, epitomizing the subjective nature of anthropogenic-based measurements. This research involves a proof-of-concept study that uses fractal indices as a means for identifying and classifying cave morphology and distinguishing genetic cave types. The fractal indices used are fractal dimension, which quantifies the complexity of a pattern, and lacunarity, which quantifies the texture of a pattern. Three-dimensional cave survey data were used to generate cave models that were converted to cave pattern image files and analyzed with image-processing software. Fractal indices were calculated for digital patterns of a limited subset of known cave types that included tafoni, littoral caves, stream caves, flank margin caves, and continental hypogene caves. The quantitative morphological distinctions in cave patterns as identified by fractal dimension and lacunarity proved to be statistically significant within the subset of cave types analyzed for this study. Similarities in geological and/or hydrogeological processes or overprinting by such processes can skew fractal indices, so geological and hydrogeological context is critical when interpreting fractal indices. The results of this study demonstrate that cave morphometry as defined by fractal indices can be used to augment the identification of cave type, which provides insight into the geological and hydrogeological controls on development of the cave type and its cavernous porosity and permeability.

Kambesis, P.N., Larson, E.B., and Mylroie, J.E., 2016, Morphometric analysis of cave patterns using fractal indices, *in* Feinberg, J., Gao, Y., and Alexander, E.C., Jr., eds., Caves and Karst Across Time: Geological Society of America Special Paper 516, p. 67–86, doi:10.1130/2016.2516(06). For permission to copy, contact editing@geosociety.org.

INTRODUCTION

Descriptive cave passage morphology has been used to distinguish among phreatic, vadose, and polygenetic cave genesis. Mylroie and Carew (1990) qualitatively described laminar recharge and its relationship to cave morphology in the coastal setting. Palmer (1991, 2007, 2011) used hydrologic recharge and structural properties of bedrock to predict descriptive morphology based on the physical layout of karstic caves and the relationship of cave passages. Roth (2004) related geometric analysis of flank margin caves of the Bahamas to cave development processes. Subsequent studies employed morphometric analyses based on similar parameters as per Roth (2004), i.e., cave area and perimeter, to determine if these parameters could differentiate between cave types (Stafford et al., 2006; Owen, 2007; Lace, 2008; Waterstrat et al., 2010). Some deviations were made from Roth's methods in that additional parameters were measured (e.g., entrance width, interior width, and inland extent). Subsequent attempts at morphometric analysis using these methods have proven to be problematic because of inconsistencies between measured parameters within morphometric data sets, nonreproducibility of statistical results, insufficient sample size, and exploration bias (Curl, 2011; Mixon, 2011; Waterstrat et al., 2011).

Cave morphometry studies typically utilize two-dimensional data sets, though some researchers have started using three-dimensional data. Labourdette et al. (2007) used three-dimensional data from the map of a Bahamian flank margin cave for conceptual modeling of karstic porosity and permeability. In an interior continental setting, Filipponi et al. (2009) used the three-dimensional geometry of complex cave systems in order to calculate statistical evidence of inception horizons, and thus relate geological setting to hydrogeological boundary conditions.

Fractal indices have been used to calculate cave length, characterize individual cave morphologies, and identify spatial distributions (Curl, 1986; Laverty, 1987; Florea and Wicks, 2001; Pardo-Igúzquiza et al., 2011, 2012). There has been limited work on the use of fractal modeling of conduit networks (Jeannin et al., 2007; Filipponi et al., 2009; Pardo-Igúzquiza et al., 2011, 2012).

Palmer (1991, 2007, 2011) quantitatively showed that mode of recharge and bedrock structural properties determined cave patterns and passage relationships in karstic caves; hence, cave morphologies are strong indicators of the processes that formed them. The goal of our research was to determine if cave patterns, such as some of those described by Palmer (2011), could be differentiated based on analysis of their fractal geometry and to ascertain if distinct cave morphologies displayed characteristic ranges of fractal indices. The fractal indices used for this study were fractal dimension, which quantifies the complexity of a pattern, and lacunarity, which quantifies the texture of a pattern (homogeneous vs. heterogeneous). Three-dimensional cave data were used to generate cave pattern images from a subset of genetic cave types including tafoni, littoral caves, stream caves, flank margin caves (coastal mixing zone), and continental hypogene caves (continental mixing zone).

Euclidean versus Fractal Geometry

In Euclidean geometry, objects are composed of points, lines, and polygons. More complex objects include planes, spheres, rectangular volumes, arcs, cylinders, etc. These objects can be classified as having an integer dimension, which is its topological dimension. This also applies to Euclidean measures such as the circumference of a circle, a curve, or the boundary of any object. A line has one-dimensional topology because one number uniquely defines any point on it. Defining a point on a two-dimensional surface can be uniquely represented by two numbers, and this is typically accomplished by gridding the surface and measuring two distances along the grid lines. The volume of an object is three-dimensional on the same basis; it takes three numbers to uniquely define any point within the object.

The mathematical description of the topological dimension in Euclidean geometry is a function of an object's change in size as the linear dimension increases (or decreases). For example, if a three-dimensional object is scaled, the volume increases by the cube of the scale factor. The relationship between topological dimension D, linear scaling L, and the resulting increase in size S is given as:

$$S = L^D. \tag{1}$$

In order to calculate topological dimension (D), the equation is rewritten as:

$$D = \log(S)/\log(L). \tag{2}$$

The equation results in an expression for topological dimension depending on how the size of the object changes as a function of linear scaling. In Euclidian geometry, the value of D is an integer depending on the actual geometry of the object (point = 1, line = 2, polygon = 3).

In mathematics and in nature, fractal morphologies do not conform to integer-based dimensionality (Bourke, 1991). The dimensions of those forms have a value that exceeds their topological dimension, and this is referred to as the fractal dimension. These are geometries that lie in a plane, but if they are linearly scaled by a factor L, the area does not increase by L^2 but by some noninteger amount. The fundamental differences between Euclidian and fractal geometries are summarized in Table 1.

Fractal Dimension and Lacunarity

The term fractal, originally coined by Benoît Mandelbrot (1983), has its root from the Latin *fractus*, meaning "broken" or "fractured." The defining properties of fractals are self-similarity and scaling, either in an exact geometric sense or in a statistical sense (Klinkenberg, 1992). Fractals in nature differ from

TABLE 1. COMPARISON OF EUCLIDEAN AND FRACTAL GEOMETRIES

Euclidean geometry	Fractal geometry
Describes simple shapes (points, lines, polygons)	Can describe geometries found in nature (irregular shapes)
Based on characteristic size or scale and a few characteristic sizes or length scales, i.e., radius of a circle, length of a side of a cube	No specifically defined size or scale; are self-similar and independent of size or scaling
Can be defined by a simple equation	Defined by algorithm

Note: Modified from Falconer (1990).

mathematically derived fractals in that the former exhibit fractal behavior over limited space and time scales, whereas the latter display infinite self-similarity and scaling (Bassingthwaighte et al., 1994).

As with other shapes and forms in nature, cave morphologies are heterogeneous and display to some degree self-similar, irregular, and fragmented geometries, which by definition make them fractals. As a consequence, the use of Euclidean-based metrics alone to define and characterize cave patterns may be a limitation in morphometric analyses.

The fractal dimension is an index used as a numerical measure of an object's complexity (surface roughness), and it reflects that object's scale invariance. It describes how an object occupies space and is related to the complexity of its structure. Sample independence or scale invariance measures have a physical significance, since the average of their spatial means does not depend on the scale (or dimension of space) over which they are averaged (Klinkenberg, 1992). Theoretically, scale invariance of fractal measures allows extrapolations from properties observed at one scale to properties of scale that have not been observed (Gilbert, 1989).

Mandelbrot (1983) noted that two fractals with different morphologies may have the same fractal dimension, so fractal dimension alone may not provide a unique morphological specification. However, there are other fractal indices that are complementary to fractal dimension. Lacunarity, which characterizes the texture of a fractal, and fractal dimension are measures that provides more detail about the pattern of a fractal, that is to say, homogeneous versus heterogeneous (Plotnick et al., 1996; Melo, 2007). Both indices are utilized in the fields of medicine, dentistry, and in physical and natural sciences (Plotnick et al., 1996; Melo, 2007).

There are a number of different methods to calculate fractal indices, including similarity dimension (Mandelbrot, 1983), Hausdorff dimension (Grassberger, 1981; Falconer, 1990), box-counting dimension (Block et al., 1990; Falconer, 1990), information dimension (Falconer, 1990), correlation dimension (Addison, 1997; Weisstein, 2006), and pointwise and average pointwise dimension (Addison, 1997). The box-counting method for determining fractal indices, originally called the Minkowski-Bouligand dimension (Falconer, 1990), can be conducted with image-processing software that calculates pixel distribution and/or density in a binarized or grayscale digital image of the object to be analyzed.

In order to calculate fractal dimension, the perimeter of an object is covered with a fixed grid of resolution δ, and the number of boxes (N) that contain pixels is counted ($N\delta$; Fig. 1). The values for N and δ are used in the following equation, which calculates topological dimension D:

$$D = [\lim \log(N\delta)], \text{ where } \delta \rightarrow 0 \log(1/\delta). \quad (3)$$

The calculations are repeated over a number of iterations using increasingly higher-resolution grids as δ goes to zero. The values for $\log(N\delta)$ are plotted against $\log(1/\delta)$, and the fractal dimension is determined by taking the slope of the line.

Lacunarity is a measure of the homogeneous versus heterogeneous texture of an object. The root of the word is from the Latin *lacuna*, which translates to "lake" or "gap." Lacunarity is a complement to fractal dimension, and it provides a textural description of a fractal (Rauch, 2007). The property of lacunarity is a function of the distribution of gaps (or holes) within the fractal. According to Mandelbrot (1983), a fractal is said to be lacunar if the gaps that it contains are large. Fractals with large gaps may also be translationally or rotationally invariant (Plotnick et al., 1996).

For this study, lacunarity was calculated with the sliding-box scanning method. The method bases its analysis on pixel density of an image that is obtained from sliding-box scanning at different box sizes and grid orientation. This method differs from the

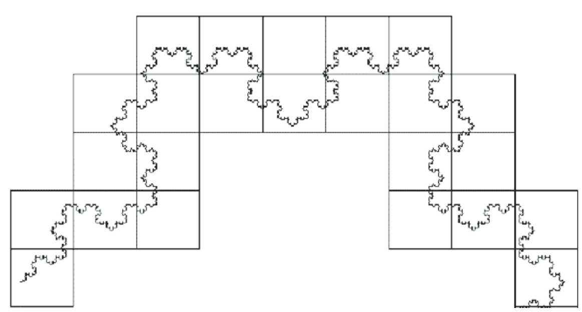

Figure 1. Box-counting method on the Koch curve.

fixed-box method used for fractal dimension, where the image is sampled only once. The equation for lacunarity calculation is

$$\lambda_{\varepsilon g} = (CV_{\varepsilon g})^2 = (\sigma/\mu)^2_{\varepsilon g}, \quad (4)$$

where λ is lacunarity, CV is the coefficient of variation (standard deviation/mean), σ is the standard deviation, and μ is the mean for pixels per box at size ε in a box count at orientation g.

The value for lacunarity is calculated using the pixel density in each ε-sized box in the grid. The lacunarity for each grid of resolution ε is then calculated from the standard deviation, σ, and mean, μ, for pixels per box. Consequently, there is a λ value for each ε in each series of grid sizes in each grid orientation g, in a set of grid orientations. A single value for lacunarity (Λ) is calculated by summarizing the values for all of the orientations and taking the average of the average (Karperien, 2013).

Degree of lacunarity is used to characterize the texture of a fractal. A high lacunarity value means that the fractal is texturally heterogeneous (Mandelbrot, 1983). Fractals with small gaps (a low lacunarity value) are classified as homogeneous (Melo, 2007). Along with the lacunarity index, descriptors of fractal texture (gappiness, heterogeneity, homogeneity, and translational or rotational invariance) can be used as modifiers to differentiate fractals that have the same or similar fractal dimension.

Since the box-counting methods use finer-resolution grids with each iteration, the precision of the fractal indices increases with each iteration as δ goes to zero. As a result, fractal indices are reported with a precision of up to 10^{-4}. This allows differentiation between similar patterns or textures. Fractal dimension and lacunarity utilized together can distinguish similar patterns.

METHODS

The indices of fractal dimension and lacunarity were calculated for 150 caves classified into five subsets of cave types (30 caves per type) that included both karstic and pseudokarstic types. The karstic cave types consisted of stream caves, flank margin caves, and continental hypogene caves from a variety of geographical locations and geological environments. Similarity of geological and/or hydrogeological processes or geologic overprinting of existing structures can result in cave patterns that are morphologically similar but genetically quite different, so geological and hydrogeological contexts were taken into consideration during this study when making interpretations based on fractal indices.

The pseudokarstic cave types were tafoni, which were exclusively from Quaternary eolianites of the Bahamas, carbonate littoral caves of the Bahamas, and noncarbonate littoral caves from the Channel Islands of California. These particular caves were chosen based on the availability of digital and hard copy maps that were of sufficient quantity and quality to allow for morphometric analysis. The dearth of such data is a reflection of the exploration bias toward small caves or ones with very limited extent and exploration potential.

The baseline data for this research were three-dimensional digital cave survey data, and cave maps whenever digital data were not available. The cave data were converted to digital images and processed via box-counting method in order to determine characteristic fractal dimension and lacunarity for each cave type. The box-counting method analyzed the complexity and texture of the perimeter of the digital cave pattern by determining pixel distribution and density over multiple iterations conducted at ever-decreasing box resolutions.

All survey data were processed with COMPASS data reduction software, which produces volumetric line plots in plan and profile view and converts them to three-dimensional shapefiles. Cave maps that were available only in hard copy were scanned and digitized using the COMPASS application Map-to-Data, which creates COMPASS data files from the digitized data. Cross sections, profiles, and known vertical extent were used to augment vertical data on digitized maps.

Cave plots were sliced into vertical increments using the COMPASS Viewer function "Set Complex: Exclude by Depth" before conversion to shapefiles. Preliminary testing indicated that slice thickness did not affect the calculation of fractal indices as long as the thickness of vertical slices was consistent. Because a significant portion of the data set included caves with less than 30 m vertical extent, 10 m slices were utilized to provide adequate vertical resolution, consistency, and speed in processing (Kambesis, 2014).

The shapefile slices were imported to ArcGIS10.2® ArcScene™ and converted to bitmap image files. Caves with vertical extent of 10 m or less were processed individually. Caves with greater vertical extent were processed as a series of bitmap images (as 10 m slices) called stacks. To calculate fractal dimension, the study used FRACTAL© version 3.4.7, which is a proprietary image-processing application that can use binary and grayscale bitmap files either individually or in stack series. Lacunarity was calculated in a stack series with FracLac, a plug-in for ImageJ, which is freeware image-processing software developed by the National Institutes of Health.

FRACTAL© version 3.4.7 and FracLac were used to analyze digital images using multiple iterations of box-counting and sliding-box-counting functions, respectively. FRACTAL was used to calculate the fractal dimension with a grid of cubes of $(\delta)^3$. The grid was placed on an image, the cubes that intersected the perimeter of the cave pattern were counted (*D*), and the topological dimension was calculated via Equation 3. In the next iteration, the resolution of the grid was reduced, and the image was reprocessed; iterations continued as the limit δ went to zero. The values for topological dimension were plotted on a log-log graph, and the fractal dimension was calculated by taking the slope of the line defined by the plotted *D* values.

FracLac was used to calculate lacunarity with the sliding-box-counting method, which is similar to that used in FRACTAL 3.4.1, though each cube (of size ε) in the grid sampled pixel distribution within the cube rather than just pixel presence. Over multiple iterations, lacunarity for each grid of size ε was calculated from the standard deviation, σ, and mean, μ, for pixels per box. This produced a lacunarity value (λ) for each ε in each series of grid sizes in each grid orientation *g*. In order to get a single value for lacunarity (Λ), a summarized value for all of the orientations was calculated by taking the average of the average (Karperien, 2013).

The box-counting applications used by FRACTAL 3.4.1 and FracLac report fractal indices to a precision of 10^{-4} in order to capture subtle variations in image pattern, though neither application provides an actual uncertainty measure.

Fractal dimension and lacunarity values were exported to Sigmaplot™ for descriptive statistics and for statistical analyses. Descriptive statistics were generated in order to determine the range (spread) of fractal dimension and lacunarity values within each cave type. The range values from the descriptive statistics were of interest because they represent variations in cave pattern and texture within a cave type.

The Shapiro-Wilk test was run on the data set to test for normality. Because the data did not pass normality testing, the nonparametric Kruskal-Wallis one-way analysis of variance by ranks was used to determine if there were statistically significant differences in fractal indices between cave types. The post hoc Student-Newman-Keuls test was conducted to locate the significant differences between the different cave types for both fractal indices.

Linear regression tests were conducted on the data set for each cave type in order to determine if there was a relationship between lacunarity (dependent variable) and fractal dimension (independent variable).

RESULTS

The quantitative morphological distinctions in cave patterns of the cave types analyzed in this study proved to be statistically significant, so the implications are that cave morphometry as defined by fractal indices may help to identify the geological and hydrogeological controls on the development of caves and cavernous porosity and permeability.

Descriptive Statistics

The descriptive statistical indices of range, maximum, minimum, mean, median, and 25th and 75th percentile are listed in Table 2A for fractal dimension by cave type and for all cave types, and in Table 2B for lacunarity of each cave type and for all cave types.

Cave patterns increase in complexity as fractal dimension increases, as illustrated in Figure 2, which is a scatter plot of fractal indices sorted on ascending fractal dimension within each cave type. Continental hypogene patterns displayed the most

TABLE 2. SUMMARY OF DESCRIPTIVE STATISTICS OF FRACTAL DIMENSION AND LACUNARITY OF EACH CAVE TYPE

A	Fractal dimension*	Tafoni	Littoral	Stream	Flank margin	Continental hypogene
	Range	0.0793	0.1870	0.1913	0.2543	0.3730
	Maximum	2.0793	2.1792	2.2984	2.5352	2.6791
	Minimum	2.0000	2.0124	2.1071	2.2830	2.3011
	Mean	2.0180	2.0749	2.2100	2.3630	2.4164
	Median	2.0100	2.0712	2.2078	2.3619	2.4271
	25th percentile	2.0010	2.0364	2.1741	2.3250	2.3770
	75th percentile	2.0293	2.0973	2.2539	2.4100	2.5281
B	Lacunarity*	Tafoni	Littoral	Stream	Flank margin	Continental hypogene
	Range	0.2271	1.2124	10.0431	3.0258	2.0174
	Maximum	0.6320	1.4360	11.972	4.0192	2.7611
	Minimum	0.1121	0.2120	1.9302	0.9934	0.7440
	Mean	0.2640	0.9718	4.763	2.1442	1.4950
	Median	0.2490	1.0724	4.7274	1.9913	1.3882
	25th percentile	0.2260	0.7313	3.0433	1.6301	1.0690
	75th percentile	0.2780	1.2731	5.9182	2.3633	1.7844

*Test for normalcy: fractal dimension: W-statistic = 0.918, $P < 0.001$ indicating data are significantly different from normal; lacunarity: W-statistic = 0.762, $P < 0.001$ indicating data are significantly different from normal.

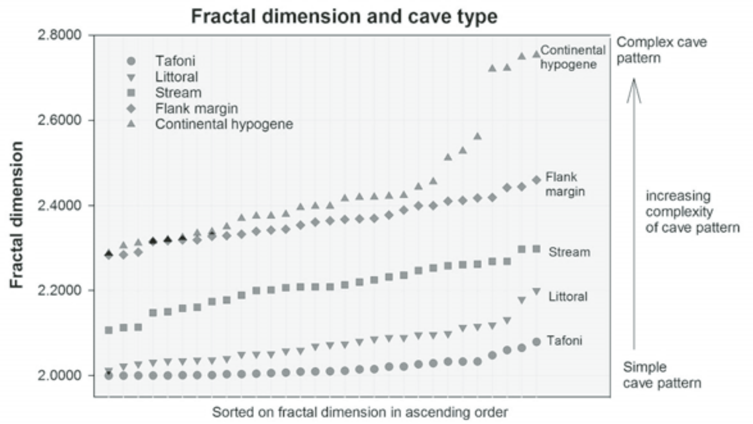

Figure 2. Comparison of cave types by fractal dimension.

complexity, while tafoni had the simplest. Flank margin pattern complexity ranked below continental hypogene pattern but above stream pattern. The littoral cave patterns analyzed in this study ranked slightly above tafoni in terms of their complexity but well below stream caves.

Figure 3A shows fractal dimension by cave type, sorted by fractal dimension, showing that fractal dimension increases with pattern complexity. Lacunarity values are shown in Figure 3B as a scatter plot sorted by fractal dimension showing that lacunarity values for individual cave patterns varied in their relationship with fractal dimension.

The range (spread) of fractal index values within each cave type is indicative of the degree of variation in passage complexity and texture within cave types (Fig. 4). Continental hypogene and stream patterns showed the largest spread in values of fractal dimension, i.e., high degree of variation in cave pattern complexity. Tafoni displayed the smallest range in fractal dimension, followed by littoral and flank margin, i.e., high degree of similarity in cave pattern complexity. Stream patterns showed the greatest variation in pattern texture, followed by flank margin and continental hypogene, respectively. Tafoni and littoral patterns displayed the narrowest spread in lacunarity, indicating little variation in pattern texture within those cave types.

Comparisons of cave patterns within each cave type are graphically shown in Figures 5 through 9. Each figure consists of a scatter plot of fractal dimension versus lacunarity (A), images of cave patterns that illustrate the range of patterns by fractal dimension and lacunarity (B), and an alphabetic list of caves analyzed within the cave type (C). Uniformity in cave pattern is illustrated by tafoni (Fig. 5) and littoral (Fig. 6) patterns. Stream cave patterns (Fig. 7) show a linear relationship between fractal dimension and lacunarity and also have the greatest range in lacunarity. Flank margin (Fig. 8) and continental hypogene patterns (Fig. 9) are characterized by the most complex cave patterns as reflected in fractal dimension values and also show significant variations in cave pattern within cave type. However, continental hypogene caves display lacunarity values that resemble those of tafoni and littoral caves.

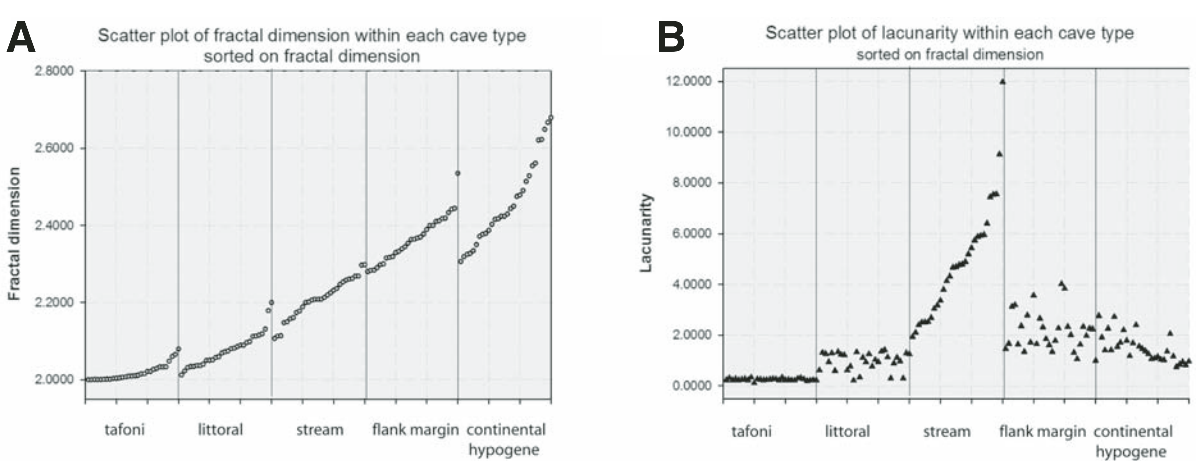

Figure 3. Scatter plots comparing fractal dimension and lacunarity by cave type.

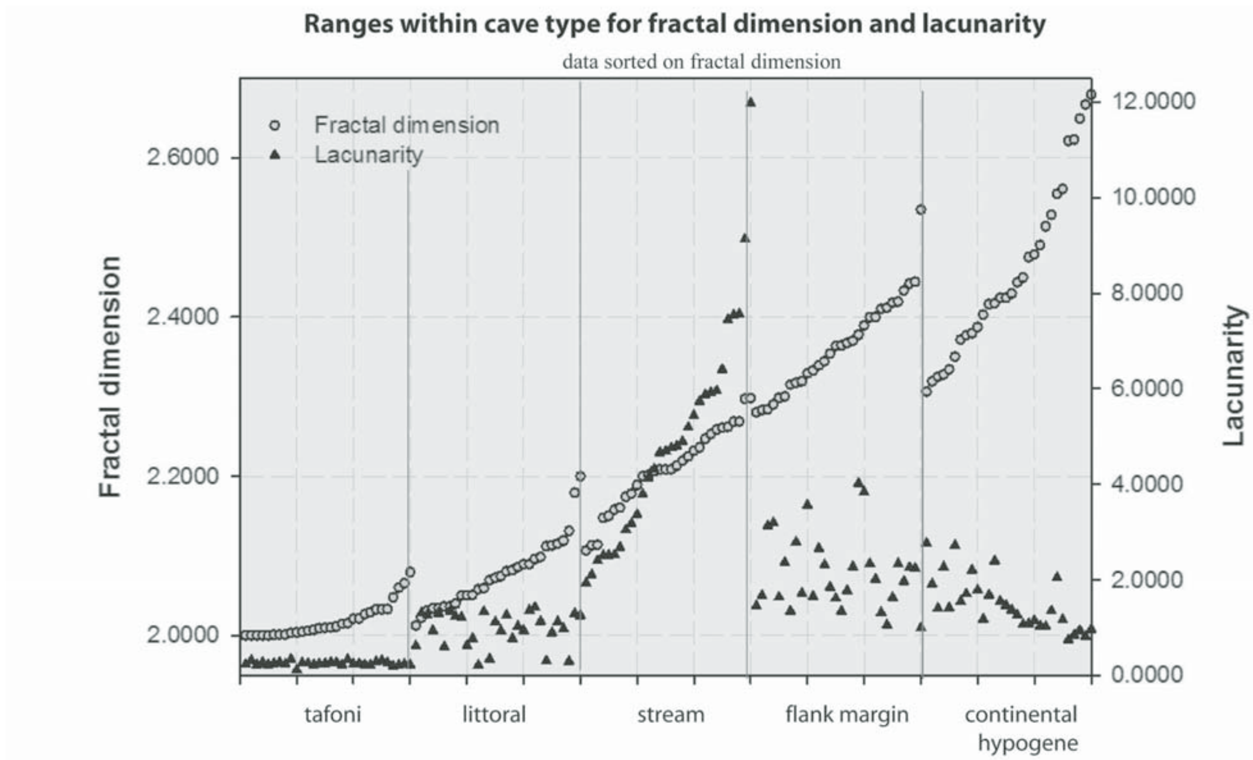

	tafoni	littoral	stream	flank margin	continental hypogene
Fractal dimension range	0.0793	0.1668	0.1913	0.2522	0.3730
Lacunarity range	0.5199	1.2240	10.0418	3.0258	2.0174

Figure 4. Combined scatter plot comparing ranges for fractal dimension and lacunarity.

The box plots of Figure 10 indicate that the fractal dimension for littoral patterns and lacunarity for stream and flank margin patterns are slightly negatively skewed. All other data are positively skewed, which is confirmed as the data do not pass normality testing. Figure 10A illustrates that fractal dimension increases with pattern complexity. Figure 10B shows that lacunarity does not always increase with fractal dimension. Stream patterns show the increasing trend of complexity and lacunarity, but flank margin and continental hypogene cave patterns do not.

Outliers were present in the fractal dimension and lacunarity box plots. Outliers in the fractal dimension plot (Fig. 10A) signify overlap in fractal dimension values due to similarity in pattern between cave types. The exceptions to this are the outliers for continental hypogene caves, which indicate extremes in pattern complexity. The most extreme outliers in lacunarity occur in steam patterns, followed by flank margin cave patterns (Fig. 10B). The other cave type patterns did not show extremes in lacunarity values.

Statistical Tests

Statistical analyses of fractal dimension and lacunarity data were conducted in order to determine if fractal indices could differentiate cave type. The data were tested for normality using the Shapiro-Wilk test; results are given at the end of Table 2. The analysis showed that the data were not normally distributed (as also indicated in the box plots; Figs. 10A and 10B), so it was necessary to use a nonparametric test to compare between cave type patterns.

Kruskal-Wallis one-way analysis of variance by ranks is a nonparametric test that assesses whether different samples in a comparison were drawn from distributions with the same median by comparing the medians. The size of each sample set is given as N. The median represents the value of the median for individual samples (for this study, cave types). The Kruskal-Wallis test statistic (H) approximates a chi-square distribution, with $k - 1$ degrees of freedom. If the calculated value of the Kruskal-Wallis test is greater than the critical H value, this indicates the samples come from different populations.

The critical value for H with four degrees of freedom is 9.488, where $\alpha = 0.05$. The calculated values from the Kruskal-Wallis test and associated H values are summarized at the bottom of Table 3. The test indicated that the differences in the median values of each cave type were greater than would be expected by chance and that the differences are statistically significant ($P = \leq 0.001$). The Kruskal-Wallis test can determine if differences exist between samples, but it does not provide any information on where the differences occur, so a post hoc test is required to identify those differences.

Fractal Indices for tafoni

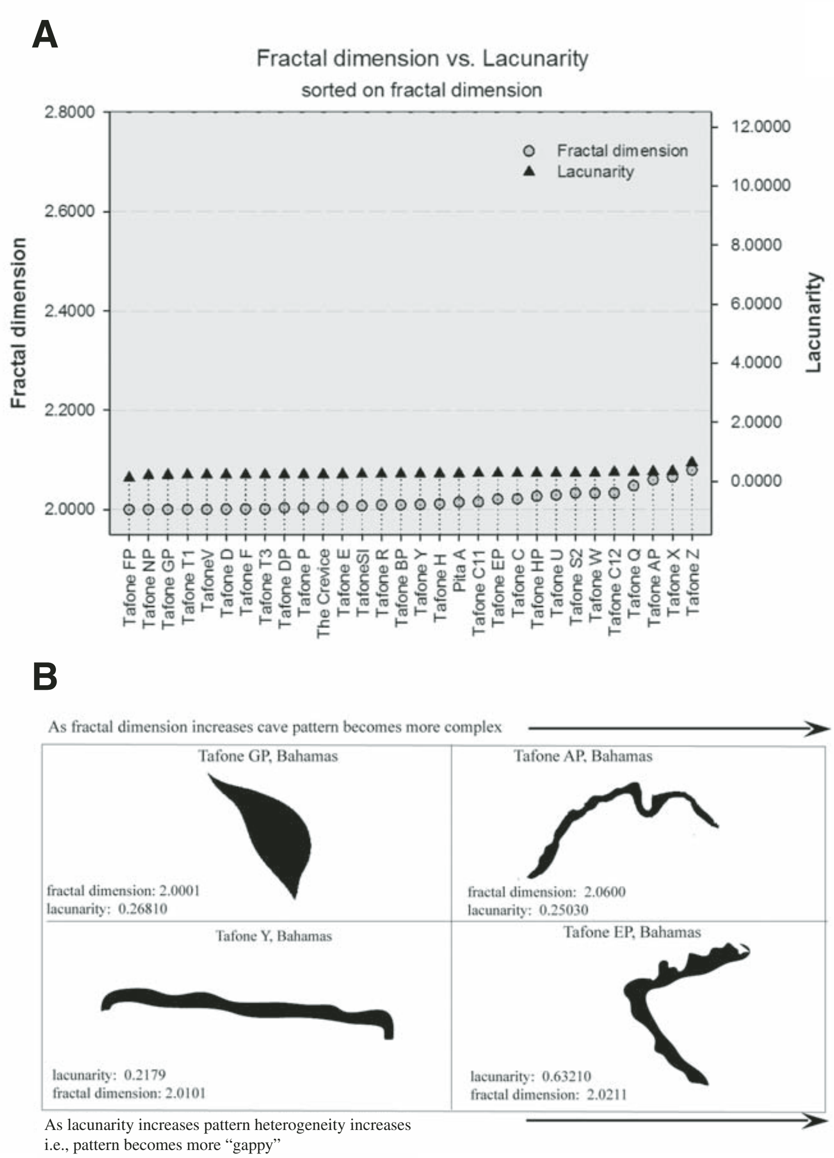

C

Cave	Location	Fractal Dimension	Lacunarity
Pita Cave A	Bahamas	2.0147	0.2212
Tafone AP	Bahamas	2.0600	0.2158
Tafone BP	Bahamas	2.0095	0.2503
Tafone C	Bahamas	2.0153	0.3302
Tafone C11	Bahamas	2.0212	0.2479
Tafone C12	Bahamas	2.0331	0.2683
Tafone D	Bahamas	2.0009	0.2467
Tafone DP	Bahamas	2.0033	0.3392
Tafone E	Bahamas	2.0060	0.2567
Tafone EP	Bahamas	2.0211	0.2332
Tafone F	Bahamas	2.0000	0.2321
Tafone FP	Bahamas	2.0012	0.2764
Tafone G	Bahamas	2.0001	0.2232
Tafone H	Bahamas	2.0112	0.2681
Tafone HP	Bahamas	2.0266	0.2272
Tafone NP	Bahamas	2.0000	0.3132
Tafone P	Bahamas	2.0036	0.1119
Tafone Q	Bahamas	2.0478	0.2000
Tafone R	Bahamas	2.0091	0.2391
Tafone S2	Bahamas	2.0329	0.2870
Tafone S1	Bahamas	2.0072	0.2262
Tafone T1&2	Bahamas	2.0001	0.2694
Tafone T3	Bahamas	2.0012	0.2352
Tafone U	Bahamas	2.0291	0.2122
Tafone V	Bahamas	2.0001	0.2219
Tafone W	Bahamas	2.0329	0.3178
Tafone X	Bahamas	2.0653	0.2339
Tafone Y	Bahamas	2.0101	0.2771
Tafone Z	Bahamas	2.0793	0.2179
The Crevice	Bahamas	2.0046	0.2617

Figure 5. Fractal indices for tafoni: (A) Scatter plot of fractal dimension vs. lacunarity. (B) Cave pattern comparisons. (C) Alphabetical list of caves analyzed.

The post hoc test used for this study was the Student-Newman-Keuls test, which is a stepwise multiple comparisons method used to identify sample means that are significantly different from each other (Shaffer, 2007). This test is used when a significant difference has been detected between three or more sample means by an a priori analysis of variance test. The method calculates a *q* value (Studentized range) by taking the difference between two sample means and dividing it by the standard error.

Fractal dimension and lacunarity were analyzed to compare each set of cave type patterns. The data showed statistically significant differences between all sets of cave type patterns, though some sets were more different than others. The cave pattern pairs with the largest difference of ranks (DoR) values in fractal dimension showed the greatest difference in cave pattern complexity. Cave patterns with largest DoR for lacunarity showed the greatest difference in the texture of a pattern. Table 4 lists the pairwise comparison of cave types by fractal dimension (A) and lacunarity (B).

For fractal dimension (Table 4A), the largest DoR values come from comparing pseudokarstic versus karstic cave patterns, Fractal Indices for littoral caves

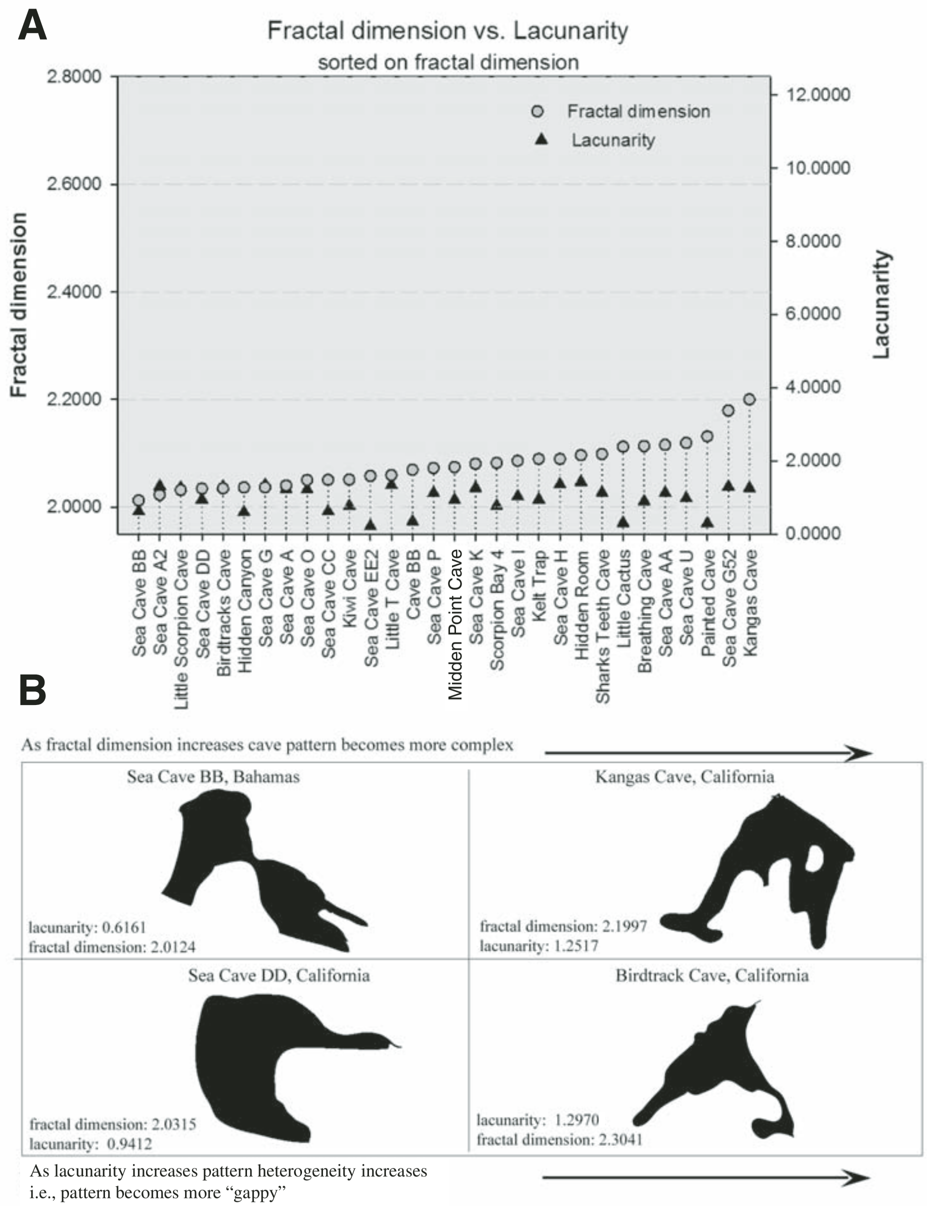

C

Cave	Location	Fractal dimension	Lacunarity
Birdtracks Cave	California	2.0344	1.2970
Breathing Cave	California	2.1132	0.8899
Cave BB	Bahamas	2.0692	0.3415
Hidden Canyon	California	2.0363	0.5959
Hidden Room	California	2.0960	1.4236
Kangas Cave	California	2.1997	1.2517
Kelt Trap	California	2.0893	0.9396
Kiwi Cave	California	2.0510	0.7681
Little Cactus	California	2.1120	0.3017
Little Scorpion	California	2.0315	1.2662
Little T Cave	California	2.0593	1.3341
Midden Pt. Cave	California	2.0743	0.9316
Painted Cave	California	2.1312	0.2963
Scorpion Bay 4	California	2.0819	0.7685
Sea Cave A	Bahamas	2.0400	1.2331
Sea Cave A2	Bahamas	2.0224	1.3067
Sea Cave AA	Bahamas	2.1154	1.1190
Sea Cave BB	Bahamas	2.0124	0.6161
Sea Cave CC	Bahamas	2.0504	0.6183
Sea Cave DD	Bahamas	2.0341	0.9412
Sea Cave EE2	Bahamas	2.0578	0.2117
Sea Cave G	Bahamas	2.0365	1.3378
Sea Cave G52	Bahamas	2.1792	1.2916
Sea Cave H	Bahamas	2.0893	1.3579
Sea Cave I	Bahamas	2.0859	1.0282
Sea Cave K	Bahamas	2.0804	1.2575
Sea Cave O	Bahamas	2.0500	1.2160
Sea Cave P	Bahamas	2.0725	1.1160
Sea Cave U	Bahamas	2.1190	0.9733
Sharks Teeth Cave	California	2.0985	1.1320

Figure 6. Fractal indices for littoral caves: (A) Scatter plot of fractal dimension vs. lacunarity. (B) Cave pattern comparisons. (C) Alphabetical list of caves analyzed.

Fractal indices for stream caves

A

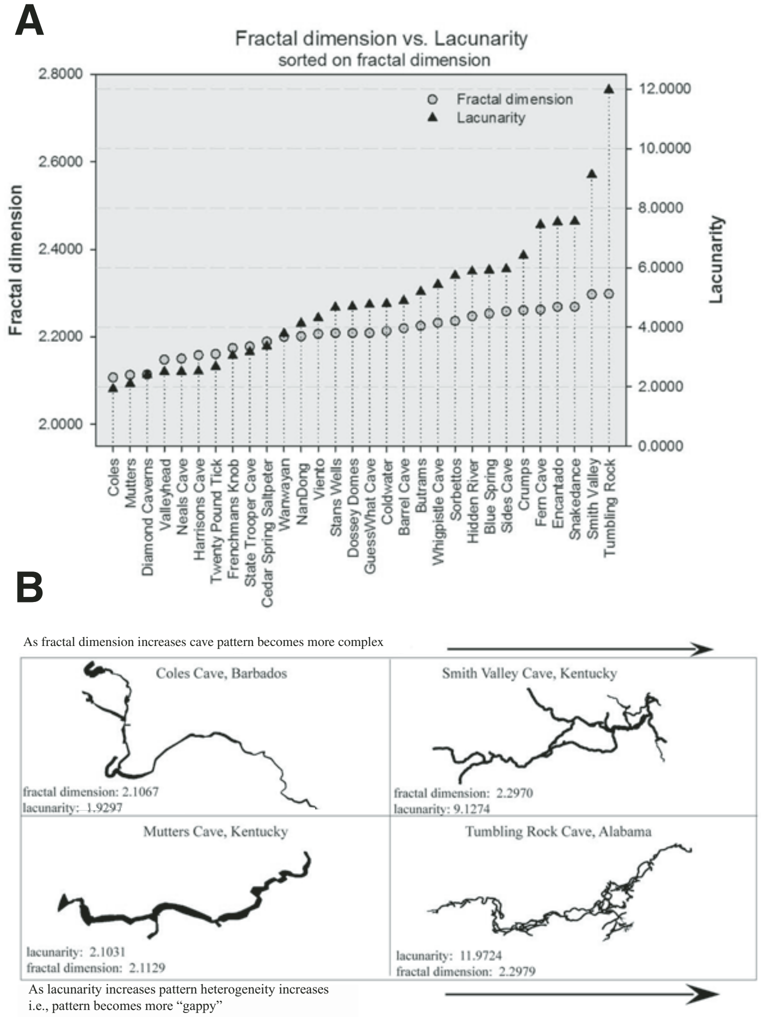

C

Cave	Location	Fractal dimension	Lacunarity
Barrel Cave	Alabama	2.2196	4.8925
Blue Spring	Tennessee	2.2530	5.9179
Butrams	Kentucky	2.2249	5.1906
Cedar Spring SP	Kentucky	2.1889	3.3625
Coldwater	Iowa	2.2132	4.7921
Coles	Barbados	2.1067	1.9297
Crumps	Kentucky	2.2608	6.4036
Diamond Caverns	Kentucky	2.1138	2.4032
Dossey Domes	Kentucky	2.2083	4.6926
Encantado	Puerto Rico	2.2683	7.5389
Fern Cave	Alabama	2.2620	7.4409
Frenchmans Knob	Kentucky	2.1741	3.0433
GuessWhat Cave	Alabama	2.2086	4.7610
Harrisons Cave	Barbados	2.1579	2.5198
Hidden River	Colorado	2.2469	5.8743
Mutters	Kentucky	2.1129	2.1031
NanDong	China	2.2013	4.1295
Neals Cave	Kentucky	2.1500	2.5106
Sides Cave	Kentucky	2.2584	5.9563
Smith Valley	Kentucky	2.2970	9.1274
Snakedance	Tennessee	2.2685	7.5574
Sorbettos	Puerto Rico	2.2360	5.7372
Stans Wells	Kentucky	2.2082	4.6613
State Trooper	Kentucky	2.1778	3.1736
Tumbling Rock	Alabama	2.2979	11.9724
Twenty LB Tick	Colorado	2.1606	2.6781
Valleyhead	Barbados	2.1476	2.5045
Viento	Puerto Rico	2.2065	4.3173
Wanwayan	China	2.2000	3.7915
Whigpistle Cave	Kentucky	2.2319	5.4351

Figure 7. Fractal indices for stream caves: (A) Scatter plot of fractal dimension vs. lacunarity. (B) Cave pattern comparisons. (C) Alphabetical list of caves analyzed.

i.e., tafoni versus continental hypogene, flank margin, and stream; and littoral versus hypogene, flank margin, and stream. Tafoni versus continental hypogene had the greatest DoR value, which is expected since they are both on the extreme ends of pattern complexity, i.e., tafoni with the simplest versus continental hypogene with the most complex. Smaller relative DoR values were displayed within karstic cave patterns (stream vs. hypogene and flank margin) and within pseudokarstic cave patterns (tafoni vs. littoral). Tafoni versus littoral, and continental hypogene versus flank margin patterns displayed the lowest DoR values for groups with significant differences.

The results of the Student-Newman-Keuls test for lacunarity are summarized in Table 4B. The clear karstic-pseudokarstic distinction seen in fractal dimension is not as prominent in DoR values for lacunarity. Stream and tafoni patterns showed the biggest difference in lacunarity and hence texture, with stream patterns expressing heterogeneous pattern texture versus tafoni showing very homogeneous patterns. The DoR values for tafoni versus flank margin and continental hypogene, and stream versus littoral and continental hypogene all indicate significant differences in lacunarity between those cave type patterns. The textures that are least different (as indicated by the lowest DoR values) are continental hypogene versus littoral, and flank margin versus continental hypogene, respectively, as their patterns trend toward homogeneous.

The lacunarity of continental hypogene patterns is surprisingly low and likely results from the dense pattern configuration displayed by three-dimensional maze patterns, which gives them a homogeneous texture. The low lacunarity value of littoral patterns results from their very simple pattern, which

Fractal Indices for flank margin caves

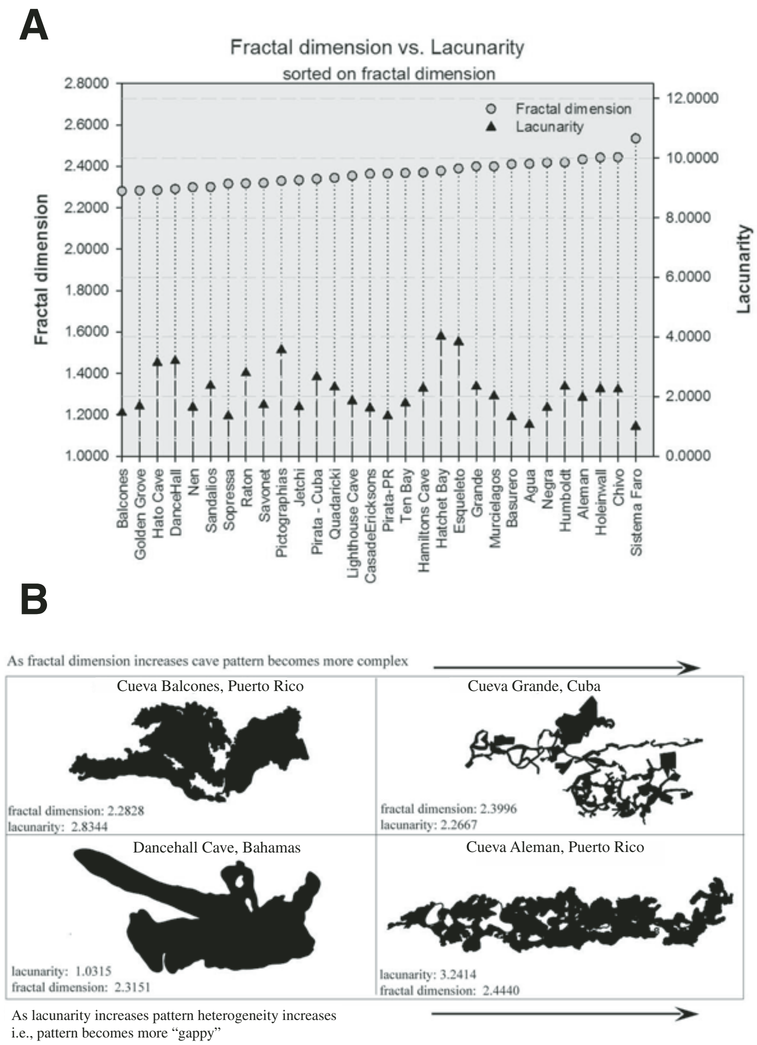

C

Cave	Location	Fractal dimension	Lacunarity
Agua	Puerto Rico	2.4116	1.0568
Aleman	Puerto Rico	2.4331	1.9712
Balcones	Puerto Rico	2.2801	1.4570
Basurero	Puerto Rico	2.4102	1.3112
CasadeEricksons	Puerto Rico	2.3635	1.6121
Chivo	Cuba	2.4440	2.2375
DanceHall	Bahamas	2.2900	3.1895
Esqueleto	Puerto Rico	2.3892	3.8331
Golden Grove	Barbados	2.2828	1.6721
Grande	Cuba	2.3994	2.3338
Hamiltons Cave	Bahamas	2.3698	2.2722
Hatchet Bay	Bahamas	2.3776	4.0189
Hato Cave	Curacao	2.2840	3.1286
Holeinwall	Bahamas	2.4418	2.2606
Humboldt	Cuba	2.4189	2.3338
Jetchi	Curacao	2.3326	1.6521
Lighthouse Cave	Bahamas	2.3537	1.8486
Murcielagos	Puerto Rico	2.3996	2.0110
Negra	Puerto Rico	2.4177	1.6300
Nen	Cuba	2.2982	1.6370
Pictographias	Cuba	2.3291	3.5644
Pirata - Cuba	Cuba	2.3391	2.6550
Pirata-PR	Puerto Rico	2.3642	1.3494
Quadaricki	Aruba	2.3442	2.3133
Raton	Curacao	2.3171	2.7868
Sandalios	Cuba	2.3001	2.3631
Savonet	Curacao	2.3191	1.7174
Sistema Faro	Puerto Rico	2.5346	0.9932
Sopressa	Puerto Rico	2.3151	1.3468
Ten Bay	Bahamas	2.3672	1.7773

Figure 8. Fractal indices for flank margin caves: (A) Scatter plot of fractal dimension vs. lacunarity. (B) Cave pattern comparisons. (C) Alphabetical list of caves analyzed.

also expresses a homogeneous texture. This situation illustrates the value of using two independent fractal indices to describe cave type patterns, e.g., continental hypogene patterns will display high fractal dimension and low lacunarity, and littoral cave patterns will display low fractal dimension and low lacunarity values.

Linear regressions were conducted to determine if there was a relationship between fractal dimension (independent variable) and lacunarity (dependent variable). Figure 11 displays a series of graphs illustrating the results of the regression analyses for each cave type. The cave type patterns where fractal dimension and lacunarity showed a relationship were stream cave patterns, which gave an $r^2 = 0.85$, and continental hypogene cave patterns, with $r^2 = 0.47$ (Figs. 11C and 11E). Tafoni had r^2 values at 0.05 (Fig. 11A). The patterns with the lowest values were flank margin patterns, with $r^2 = 0.016$, and littoral, at $r^2 = 0.001$ (Figs. 11D and 11B).

DISCUSSION

It is mathematically interesting to note how image patterns representing different cave types can be described and distinguished by fractal indices. What would be of greater value is if fractal indices could augment the identification, description, and classification of cave morphologies for the purpose of understanding hydrologic function and speleogenetic process. In order to serve this function, fractal indices must be considered within the context of geography, geology, and hydrology; otherwise, Fractal Indices for continental hypogene caves

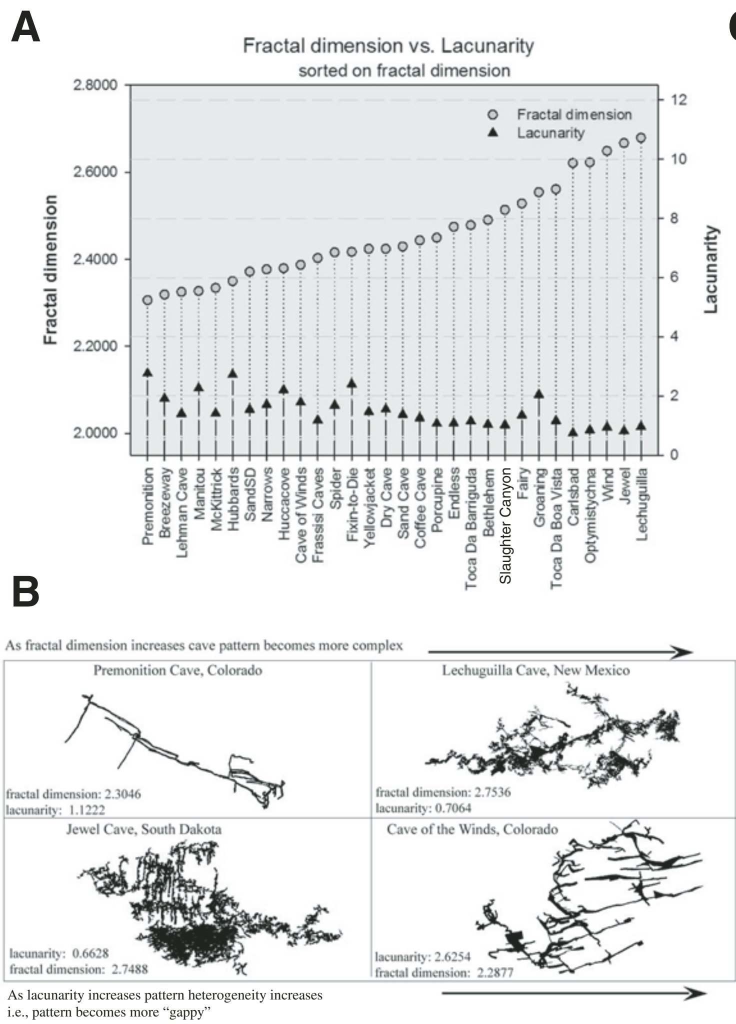

C

Cave	Location	Fractal dimension	Lacunarity
Bethlehem	South Dakota	2.4902	1.0373
Breezeway	Colorado	2.3189	1.9122
Carlsbad	New Mexico	2.6208	0.7443
Cave of Winds	Colorado	2.3870	1.7841
Coffee Cave	New Mexico	2.4434	1.2600
Dry Cave	New Mexico	2.4238	1.5529
Endless	New Mexico	2.4748	1.0795
Fairy	Colorado	2.5282	1.3524
Fixin-to-Die	Colorado	2.4168	2.3991
Frassisi Caves	Italy	2.4026	1.1803
Groaning	Colorado	2.5542	2.0456
Hubbards	Colorado	2.3499	2.7206
Huccacove	Colorado	2.3792	2.2028
Jewel	South Dakota	2.6667	0.8175
Lechuguilla	New Mexico	2.6792	0.9623
Lehman Cave	Nevada	2.3249	1.4030
Manitou	Colorado	2.3274	2.2641
McKittrick	New Mexico	2.3340	1.4114
Narrows	Colorado	2.3768	1.7074
Optymistychna	Ukraine	2.6225	0.8469
Porcupine	South Dakota	2.4494	1.0687
Premonition	Colorado	2.3060	2.7612
Sand Cave	New Mexico	2.4293	1.3740
SandSD	South Dakota	2.3714	1.5456
Slaughter Canyon	New Mexico	2.5136	1.0209
Spider	New Mexico	2.4158	1.6842
Toca da Barriguda	Brazil	2.4784	1.1478
Toca da Boa Vista	Brazil	2.5608	1.1612
Wind	South Dakota	2.6488	0.9407
Yellowjacket	New Mexico	2.4238	1.4645

Figure 9. Fractal indices for continental hypogene caves: (A) Scatter plot of fractal dimension vs. lacunarity. (B) Cave pattern comparisons. (C) Alphabetical list of caves analyzed.

they are just a collection of numbers that describe image patterns. The following paragraphs consider geographic, geological, and hydrogeological context in the discussion of each cave type and their associated patterns and textures.

Tafoni

Tafoni analyzed in this study are located in Pleistocene and Holocene eolianites of the Bahamas. Geographically, the tafoni were distributed between San Salvador, Little Abaco, and Long Islands. Bahamian tafoni are pseudokarstic features that formed on cliffed surfaces that were subsequently exposed to mild wind erosion but out of the reach of sea spray (Owen, 2007, 2013). The geographic locations are restricted, and the variation in conditions under which they form is narrow. Consequently, Bahamian tafoni display the simplest of cave patterns and were the least variable in morphology as indicated in their narrow range of fractal indices (Fig. 5). Their simple morphology also gives them a homogeneous texture, reflected in the lowest lacunarity values of all of the cave types in this study. However, the tafoni patterns in this study showed no relationship between fractal dimension and lacunarity ($r^2 = 0.05$; Fig. 11A). The tafoni patterns analyzed in this study represented tafoni from different locations on four different islands, so the degree of weathering may be a factor in the textural morphology of these features as quantified by lacunarity. There was not a consistent enough distribution of tafoni in each site to try and compare fractal dimension versus lacunarity within and between sites.

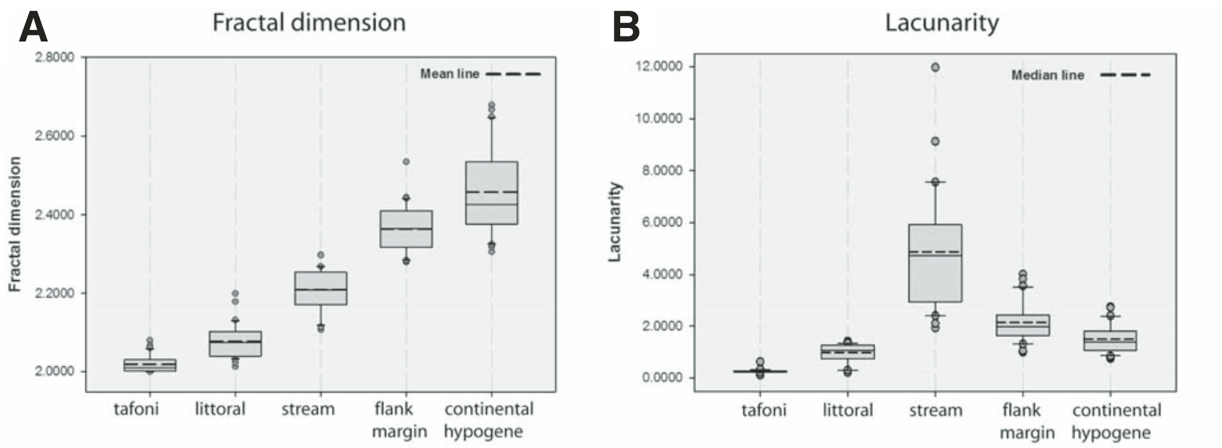

Figure 10. Box plots for fractal indices.

Littoral Caves

Littoral caves are pseudokarstic features formed by the erosional action of waves on a coastline. The littoral caves analyzed in this study came from only two geographic locations, the Channel Islands of California, USA, and the Bahamas. Cave development in these areas is restricted to coastal zones, though the rock types did vary from strictly carbonates in the Bahamas to igneous rocks on the Channel Islands.

The littoral cave patterns analyzed in this study were simple in form, though not as simple as tafoni (Fig. 6). Their range in fractal dimension and lacunarity values was slightly above tafoni. Littoral caves form by one overall process, which is wave action on a coastline. However, there is a degree of latitude in terms of the range of littoral cave patterns as a function of configuration of coastline and variations in rock structures and lithologies. As with tafoni, regression analysis of fractal dimension versus lacunarity was very low (Fig. 11B). Degrees of overprinting by other erosional processes are common in the littoral cave environment, and this could randomly affect the textural morphology of cave patterns.

Stream Caves

The sample of stream caves analyzed in this study had wide geographic distribution (Kentucky = 14, Alabama-Tennessee = 6, Colorado = 1, Iowa = 1, and international locations that include Barbados, China, Cuba, and Puerto Rico.) By definition, stream caves are karstic, and the ones analyzed for this study had recharge modes of either sinking streams, sinkholes or both. In complexity of cave pattern, stream caves rank well above littoral patterns but below flank margin patterns. The stream caves analyzed in this study were predominantly linear in form (i.e., branchwork; Fig. 7). The more extensive stream systems displayed complex local patterns attributable to the occurrence of floodwater mazes that can form at restrictions, breakdown or sediment distribution

TABLE 3. KRUSKAL-WALLIS ONE-WAY ANALYSIS OF VARIANCE ON RANKS TEST DETERMINING THAT FRACTAL INDICES OF CAVE TYPE PATTERNS ARE STATISTICALLY DIFFERENT

		Cave types				
A	Fractal dimension	Tafoni	Littoral	Stream	Flank margin	Continental hypogene
	N	30	30	30	30	30
	Median	2.0101	2.0731	2.2083	2.3642	2.4027
	25th percentile	2.0014	2.0400	2.1744	2.3177	2.3770
	75th percentile	2.0306	2.0993	2.2534	2.4101	2.5280
B	Lacunarity	Tafoni	Littoral	Stream	Flank margin	Continental hypogene
	N	30	30	30	30	30
	Median	0.2489	1.0724	4.7271	1.9913	1.3883
	25th percentile	0.2264	0.7688	3.0432	1.6300	1.0687
	75th percentile	0.2771	1.2667	5.9187	2.3635	1.7844

Note: Test statistic H = 132.858 (fractal dimension); H = 123.257 (lacunarity) with four degrees of freedom (df) (P = <0.001). N is number of caves within each cave type in this study; median is for each cave type in the study data set for fractal index (fractal dimension and lacunarity).

TABLE 4. POST HOC STUDENT-NEWMAN-KEULS TEST INDICATES STATISTICAL DIFFERENCE BETWEEN CAVE PATTERNS USING FRACTAL INDICES

Comparison of cave types	Difference of ranks (DoR)	q^*	P	$P < 0.050$
A. Fractal dimension (sorted on DoR)				
Continental hypogene vs. tafoni	3328.00	13.9991	<0.001	Yes
Flank margin vs. tafoni	2829.00	14.8482	<0.001	Yes
Continental hypogene vs. littoral	2532.00	13.2900	<0.001	Yes
Flank margin vs. littoral	2032.00	14.2010	<0.001	Yes
Stream vs. tafoni	1710.00	11.9500	<0.001	Yes
Continental hypogene vs. stream	1619.00	11.3140	<0.001	Yes
Flank margin vs. stream	1119.00	11.6980	<0.001	Yes
Stream vs. littoral	913.00	9.5450	<0.001	Yes
Littoral vs. tafoni	797.00	8.3320	<0.001	Yes
Continental hypogene vs. flank margin	500.00	5.22270	<0.001	Yes
B. Lacunarity (sorted on DoR)				
Stream vs. tafoni	3459.00	14.5360	<0.001	Yes
Flank margin vs. tafoni	2475.00	12.9990	<0.001	Yes
Stream vs. littoral	2394.00	12.5650	<0.001	Yes
Continental hypogene vs. tafoni	1791.00	12.5170	<0.001	Yes
Stream vs. continental hypogene	1668.00	11.6570	<0.001	Yes
Flank margin vs. littoral	1410.00	9.8540	<0.001	Yes
Littoral vs. tafoni	1065.00	11.1340	<0.001	Yes
Stream vs. flank margin	984.00	10.2870	<0.001	Yes
Continental hypogene vs. littoral	726.00	7.5900	<0.001	Yes
Flank margin vs. continental hypogene	684.00	7.1510	<0.001	Yes

Note: q^* is the Studentized range, which is the difference between the largest and smallest data within each cave type, measured in units of sample standard deviations.

that affects water flow, and/or in their multilevel development due to changes in base level, which adds a vertical maze component to their morphology.

Stream caves not only display the greatest range in lacunarity, but they also show that increase in stream pattern lacunarity is directly related to increase in stream fractal dimension ($r^2 = 0.85$). This direct correlation in indices may be related to the structural character of the bedrock in which stream caves form. Regardless of the structural control on stream caves, be it fractures, bedding planes, or intragranular pores, the morphology of the cave type is strongly linear. This condition may influence the development and evolution of morphological texture that is heterogeneous.

Flank Margin Caves

The flank margin caves analyzed in this study were all from the Caribbean region (Puerto Rico = 11, Bahamas = 7, ABC Islands = 6, Cuba = 5, Barbados = 1). Flank margin caves form as a result of the mixing of freshwater and marine water at the distal end of a freshwater lens (coastal mixing zone), which tracks the edge of a carbonate coast. Freshwater lens morphology is subtly affected by its relationship to a coastline, i.e., parallel to a linear coastline; following the trend of a coastline with changing trend; relationship to coastal embayments. Thus, flank margin cave pattern reflects lens morphology.

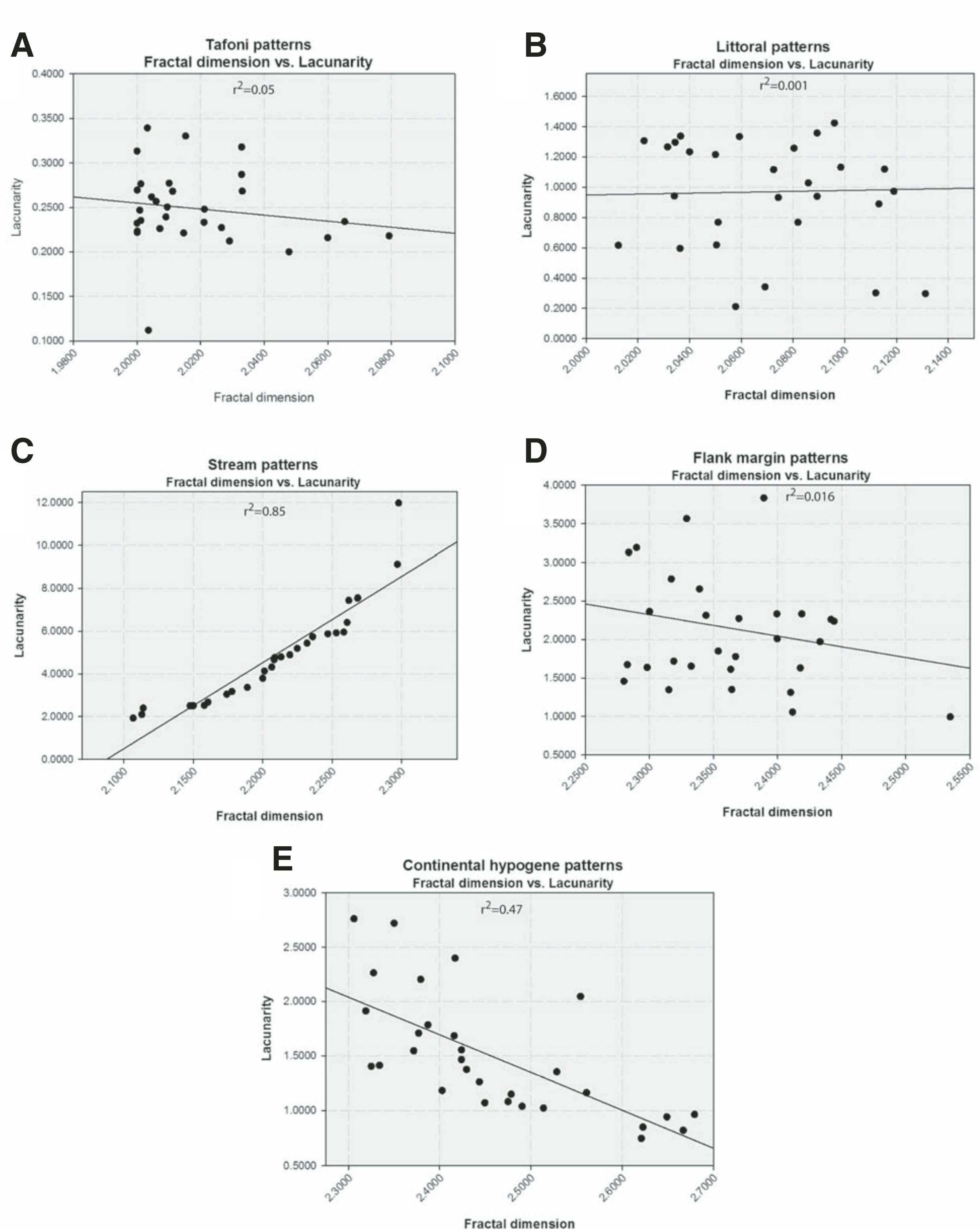

Figure 11. Results of linear regression analyses for fractal dimension vs. lacunarity.

Flank margin patterns have a more restricted fractal dimension range than stream patterns and are very close in range value to littoral caves, which may be indicative of their development in specific hydrogeological and geological conditions, i.e., at the distal margin of the freshwater lens, just under the flank of the enclosing landmass (Mylroie and Mylroie, 2007), and in coastal rock types characterized by eogenetic structural characteristics, though they have been documented in telogenetic settings (Mylroie et al., 2008; Otoničar et al., 2010; D'Angeli et al., 2015).

Caribbean flank margin caves can have very complex morphologic footprints, but they are typically less developed in vertical extent than continental hypogene caves or stream caves. Their lacunarity values are higher than those of hypogene caves because the mazes they form are not as three-dimensionally dense and therefore are more heterogeneous in texture (Fig. 8).

Flank margin caves analyzed for this study showed no relationship between fractal dimension and lacunarity ($r^2 = 0.016$). This may be due to several factors that randomly affect pattern texture, including overprinting by coastal processes, coastal configuration, degree of karstification, or sampling bias.

Continental Hypogene Caves

The continental hypogene caves analyzed for this study came from a variety of different geographic areas (Colorado = 11, New Mexico = 11, South Dakota = 5, Nevada = 1, Brazil = 1, and Italy = 1). Palmer (2007) defined hypogene caves as ones formed by water where aggressiveness was produced at depth beneath the surface, independent of surface or soil CO_2 or other near-surface acid sources. Palmer (2007) also correlated specific patterns with specific modes of recharge, including H_2S oxidation zones, rising thermal water, and deep mixing zones, which all operate over regional hydrologic scales. The continental hypogene data for this study did not take into account the differences in recharge mode, or the structural characteristics of the bedrock that may influence patterns. This may explain the great spread in fractal dimension values, and the relationship between fractal dimension and lacunarity ($r^2 = 0.47$). The patterns with extremely high fractal dimension gave correspondingly low lacunarity values, indicating a possible inverse relationship (Fig. 9). An explanation for this may be that continental hypogene caves form dense three-dimensional mazes with a high measure of object complexity, so their texture becomes more homogeneous. It is possible that had we classified and analyzed hypogene cave patterns according to process and structural characteristics rather than randomly, a stronger relationship between the indices might have emerged, though this is highly speculative at this point.

Significance of Range (Spread) in Fractal Indices

Though fractal indices are not direct indicators of specific processes or geologic and hydrogeological conditions, they do identify patterns and ranges of patterns that may be characteristic of processes, or geological and hydrological conditions. Figure 4 shows ranges of fractal dimension and lacunarity for each cave type. The magnitude of the range may reflect the range of conditions that could have formed the pattern. A relatively narrow range in value of fractal dimension within a cave type suggests one dominant formational process. For example, tafoni and littoral caves are formed by one definitive process (weathering of cliffed surfaces in the former; wave erosion in the latter). Stream caves rank above tafoni and littoral caves in fractal dimension range and are formed by three modes of surface recharge: either by sinking streams, sinkholes, or both. Flank margin caves and continental hypogene caves display the greatest range in fractal dimension and thus the most variation in cave pattern. Flank margin caves analyzed in this study have one basic mode of recharge into several possible geologic conditions, including forming parallel to a linear coastline; following the trend of a coastline with changing trend; and forming parallel to coastal embayments. For continental hypogene caves, different hypogenetic processes (H_2S oxidation zones, rising thermal water, and deep mixing zones) may result in different cave patterns, which could explain the range in fractal dimension in the continental hypogene caves types chosen for this study.

Unlike fractal dimension, lacunarity is not definitive in terms of identifying specific cave patterns. However, it does identify variations within patterns in the form of textural differences. This suggests that ranges of lacunarity might reflect degree of process or overprinting by other processes, though one must be careful to keep geologic and hydrologic conditions in mind when considering this. The lowest values and narrowest ranges in lacunarity occur within tafoni and littoral caves, giving them a homogeneous texture. Coastal weathering or erosion, or overprinting of existing patterns by erosion from wave energy may "open" the pattern of the cave, making it gappier in appearance and thus increasing slightly the lacunarity value.

Flank margin patterns rank higher in lacunarity above tafoni and littoral patterns but much less than stream cave patterns. These cave types are also subject to coastal erosion and/or overprinting by erosion from wave energy. These conditions affect the texture of the original cave morphology by making it gappier, which is reflected in higher lacunarity values and ranges of those values within flank margin caves.

The greatest range in lacunarity values and the strongest relationship between fractal dimension and lacunarity are expressed in stream cave patterns. Stream cave morphology is strongly influenced by recharge type and by linear structural patterns that maintain their linearity as the cave evolves in morphology by corrosion, corrosion, and/or changes in base level. As the pattern of a stream cave becomes more complex, while still maintaining its linearity, the gappiness of the texture of the pattern appears to evolve with it. Thus, lacunarity increases as fractal dimension increases.

Unlike stream caves, the patterns of continental hypogene caves do not increase in lacunarity (become gappier) as the cave pattern evolves. Rather, the more complex the development of three-dimensional mazes, the more homogeneous they appear in texture, which may explain the low range of lacunarity values that are characteristic of highly developed mazes, a common morphology of many continental hypogene caves.

Geological and Hydrological Context for Pairwise Comparisons of Cave Types

Palmer (2011) effectively demonstrated that morphologies of caves are indicators of geological controls, hydrological processes, and speleogenetic mode. Though he did not address pseudokarst in the analysis, our study suggests that pseudokarstic morphologies, when considered within geologic context, can also be indicators of geological control and process. The cave types analyzed in this study included karstic and pseudokarstic types, which can be distinguished and described by fractal indices. Table 4 summarizes the pairwise comparisons of cave type patterns.

The most notable differences in cave patterns occurred between karstic versus pseudokarstic cave types. Tafoni and continental hypogene cave types showed the greatest difference in fractal dimension, followed by tafoni versus flank margin, and littoral versus hypogenetic and flank margin. This reflects the vastly different modes of cave genesis between pseudokarstic and karstic cave types.

The cave types showing the least difference in fractal dimension were continental hypogene caves versus flank margin caves and tafoni versus littoral caves, indicating similarity in formational process within the groups. Though continental hypogene and flank margin cave types developed in very different geological and hydrological conditions, both cave types initially formed in a mixing zone environment, so their overall morphologies are similar. Tafoni and littoral caves are formed by coastal-related mechanical processes (weathering vs. erosion), which may explain their similarity in morphology.

Flank margin caves and littoral caves ranked significantly different in terms of fractal dimension. Flank margin caves form by mixing zone corrosion, whereas littoral caves form by mechanical erosion. However, flank margin caves that have been exposed to erosion by wave energy may become overprinted by littoral erosion such that their pattern mimics those of littoral caves, which results in overlap in values of fractal indices between these cave types.

Stream caves were clearly differentiated from tafoni, continental hypogene, flank margin, and littoral caves in terms of fractal dimension, since the processes that form stream caves are definitively different from the processes that formed the others.

The biggest differences in lacunarity are displayed in pseudokarstic versus karstic caves. Pseudokarstic caves display simple patterns, which are homogeneous in surface texture and indicative of one formational process. The diversity of karstic cave morphologies is a reflection of variety in recharge type, variations in structural character of bedrock, and speleogenetic history. Karstic caves can express a range from simple (homogeneous) textures to complex textures that are strongly heterogeneous. Caves that display the greatest differences in cave patterns are tafoni versus stream caves and flank margin caves, and littoral caves versus stream caves.

Caves that show the least differences in lacunarity are littoral versus flank margin, and flank margin versus continental hypogene. Though littoral caves form by a mechanical process versus flank margin caves, which are dissolutional, they are both subject to continued wave erosion, which simplifies the patterns of both cave types. Flank margin and continental hypogene caves can form complex mazes, which can express homogeneous textures and low lacunarity values.

Outliers, Fractal Indices, and Geological and Hydrological Context

Similarities in geological and hydrogeological processes and/or overprinting of processes can skew fractal dimension. All five cave types in the data set displayed some degree of overlap in the values of fractal dimension. That overlap is represented by the outliers above and below the box plots for the five cave types (Fig. 12). The most prominent overlap is between flank margin and continental hypogene caves. This may result in part because both cave types are the result of mixing zone corrosion; hence, cave patterns can be similar. Flank margin caves, which by definition are coastal features, form as a result of mixing between freshwater and marine water. Continental hypogene caves, which are predominantly inland features, result from the interaction of chemically different groundwater. Geographical, geological, and hydrogeological context is critical for differentiating between the two.

Small flank margin caves and littoral caves can have very similar fractal dimensions. Flank margin caves, as noted already, may be exposed to wave energy that overprints their original complex wall morphology with the less complex wall morphology of a littoral cave. Features that help differentiate these cave types include inorganic speleothem development, remnant dissolutional features such as ceiling pendants and/or pillars, bell holes, geographic location, and elevation with respect to sea level. Extreme littoral overprinting or cliff-line erosion can make it very difficult to differentiate between highly overprinted flank margin and littoral caves.

Tafoni have the least complex of all cave wall morphologies but could potentially be confused with highly denuded littoral or flank margin caves. However, tafoni are very short lived and form well above the level of sea spray, or at sea level where sea spray is not common (quiet lagoons) so geographical as well as geological context can help differentiate these types of caves.

The cave patterns with the greatest outliers of fractal dimension within their groups all share the characteristic of being polygenetic. Caves that are polygenetic have undergone multiple stages of development, some of which may overprint earlier morphologies. Figure 12 lists specific caves analyzed in this study with the highest fractal dimensions, and these caves rank among the longest and most complex cave systems in the world.

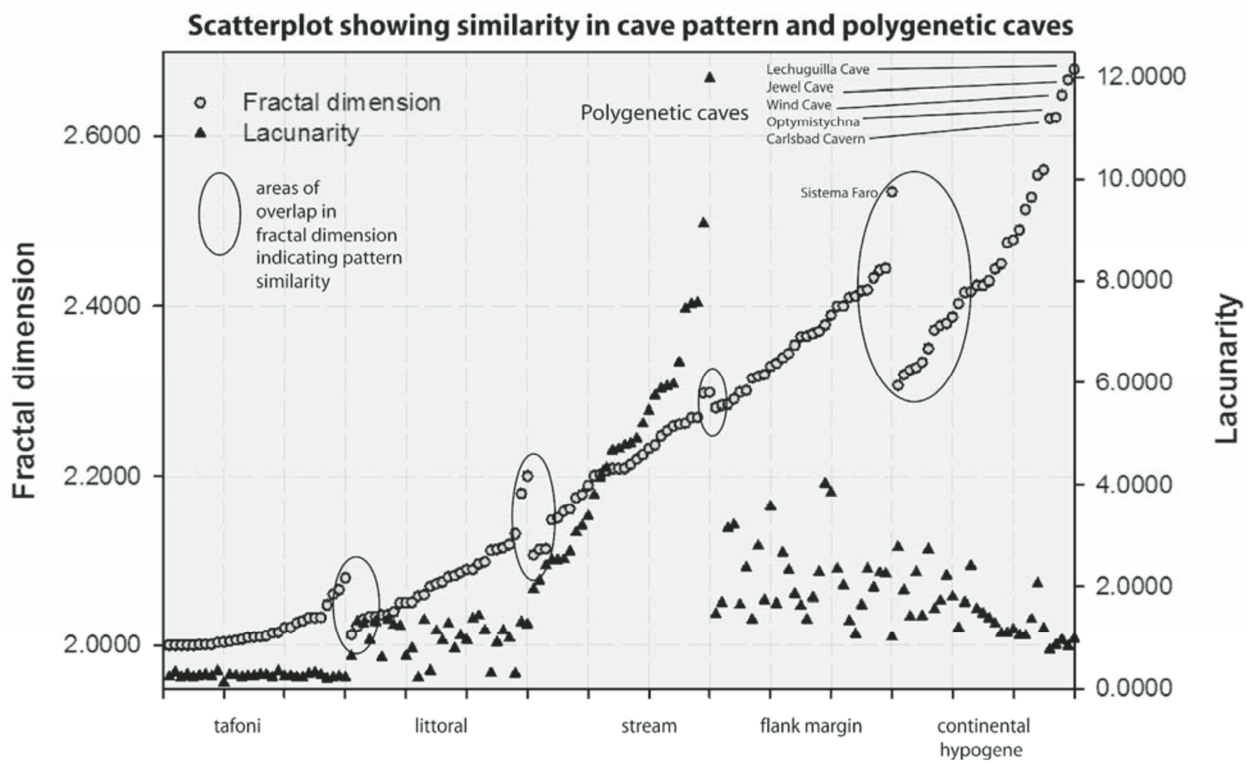

Figure 12. Scatter plot of fractal indices showing overlap in fractal dimension values between cave types, which signifies similarity of pattern. The greatest outliers from the box plots displayed in all cave types are polygenetic caves.

All caves are polygenetic to some degree, but the largest cave systems show the tendency to the extreme.

All of the patterns analyzed in this study were treated as monofractals, i.e., patterns that are described with one scaling rule. However, large, complex cave patterns should be treated as multifractals. The difference between the two fractal types is that multifractals are scaled with multiple scaling rules in order to demonstrate how scaling varies over a data set. This was beyond the scope of this particular study but will be treated in future work.

CONCLUSIONS

Fractal indices were calculated for digital patterns of a limited subset of known cave types that included tafoni, littoral caves, stream caves, flank margin caves, and continental hypogene caves. The statistical analyses, both a priori and post hoc, showed that the differences in cave patterns as identified by fractal indices proved to be significant between the subset of cave types analyzed for this study.

Fractal dimension, which quantifies degree of pattern complexity, increases as the complexity of a cave pattern increases, and it can quantitatively describe and differentiate cave patterns (Fig. 2). Continental hypogene patterns have the most complex morphologies, while tafoni have the simplest, and this is reflected in fractal dimension, which is highest for the former and lowest in the latter. Flank margin pattern complexity ranked below continental hypogene pattern but above stream pattern. The littoral cave patterns analyzed in this study ranked slightly above tafoni in terms of their complexity but well below stream caves.

Lacunarity values alone did not prove to be a stand-alone index for cave type identification. However, they did identify variations within pattern types in the form of textural differences within specific patterns (Fig. 3). Simple cave patterns are homogeneous in texture, as displayed by tafoni and littoral caves. Stream patterns displayed the highest values and ranges of lacunarity, which may be a function of their predominantly linear morphology, one that is characterized by heterogeneous textures. Maze cave patterns tend to be less heterogeneous than stream patterns, and continental hypogene patterns can display homogeneous textures due to complex three-dimensional maze development.

The range (spread) of fractal index values within each cave type is indicative of the degree of variation in passage complexity and texture within cave types (Fig. 4). A small range in value of fractal indices within a cave type suggests one dominant formational process. A wide spread of fractal indices may indicate that the cave patterns represent a variety of processes or geological/hydrogeological conditions though which process or condition is not specified.

Similarities in geological and hydrogeological processes and/or overprinting of processes can skew fractal indices, which are represented by the box plot outliers (Fig. 10). The most prominent overlap in fractal dimension values is between flank margin and continental hypogene caves, which suggests that cave patterns are similar because both are the result of mixing zone corrosion. Geological and hydrogeological context is critical for differentiating between the two. Small flank margin caves and littoral caves can have very similar fractal dimensions. Flank margin caves may be exposed to wave energy that overprints their original complex wall morphology with the less complex wall morphology of a littoral cave. Extreme littoral overprinting or cliff-line erosion can make it extremely difficult to differentiate between overprinted flank margin and littoral caves.

Regression analyses between fractal dimension (independent variable) and lacunarity (dependent variable) showed a strong relationship within stream patterns and to a lesser degree within continental hypogene caves. The other cave types did not show a relationship between fractal dimension and lacunarity (Fig. 11).

The cave patterns with the highest fractal dimension within their groups all share the characteristic of being polygenetic, and this is expressed in the outliers (Figs. 10 and 12). Polygenetic caves are the result of multiple stages and sometimes multiple processes of cave development. All caves are polygenetic to some degree, but the largest and oldest cave systems show that tendency to the extreme and should be treated as multifractals.

Summary

This study was a proof-of-concept for the idea that fractal indices could be used to describe and differentiate cave types. The method for determining fractal indices involved converting three-dimensional cave data to digital images that were analyzed by pattern recognition software. Fractal indices were calculated using box-counting algorithms. The quantitative morphological distinctions in cave patterns as identified by fractal dimension and lacunarity proved to be statistically significant within the subset of cave types analyzed for this study.

Fractal indices do not define process or predict speleogenetic outcomes, but they do identify cave patterns that are characteristic of specific processes and speleogenetic conditions. As long as geological and hydrogeological context are taken into consideration, cave pattern morphology as described by fractal indices could be used to augment the identification and differentiation of karstic processes and conditions that formed them.

ACKNOWLEDGMENTS

We wish to acknowledge support from the Department of Geoscience at Mississippi State University, Exxon-Mobil, Cave Research Foundation, and the National Speleological Foundation. We would like to thank Carlsbad Caverns National Park, Jewel Cave National Monument, Wind Cave National Park, and Mammoth Cave National Park for providing a portion of the data used in this study, and the following individuals and groups for providing data sets: Paul Burger, Dave Bunnell, Mike Lace, Marc Ohms, Athena Owen-Nagel, Coldwater Cave Project, Cuba Caves Project, Fern Cave Project, Isla de Mona Project, and Whigpistle Project. Thanks also go to Aaron Addision for providing geographic information system advice and support. Finally, we appreciate the reviews and comments of two anonymous reviewers, which helped to improve the manuscript.

REFERENCES CITED

Addison, P.S., 1997, Fractals and Chaos: An Illustrated Course: Bristol, UK, Institute of Physics Publishing, 256 p.

Bassingthwaighte, J.B., Liebovitch, L.S., and West, B.J., 1994, Fractal Physiology: New York, Oxford University Press, 364 p.

Block, A., von Bloh, W., and Schellnhuber, H.J., 1990, Efficient box-counting determination of generalized fractal dimension: Physical Review A, v. 42, no. 4, p. 1869–1874, doi:10.1103/PhysRevA.42.1869.

Bourke, P., 1991, An Introduction to Fractal: http://paulbourke.net/fractals/fracintro/ (accessed August 2014).

Curl, R.L., 1986, Fractal dimensions and geometries of caves: Mathematical Geology, v. 18, no. 8, p. 765–783, doi:10.1007/BF00899743.

Curl, R., 2011, Comment on "Coastal Caves in Bahamian eolian calcarenites: Differentiating between sea caves and flank margin caves using quantitative morphology": Journal of Cave and Karst Studies, v. 73, no. 3, p. 202, doi:10.4311/jcks2011es0195.

D'Angeli, I.M., Sanna, L., Calzoni, C., and De Waele, J., 2015, Uplifted flank margin caves in telogenetic limestone in the Gulf of Orosei (central-east Sardinia-Italy) and their paleogeographic significance: Geomorphology, v. 231, p. 202–211, doi:10.1016/j.geomorph.2014.12.008.

Falconer, K., 1990, Fractal Geometry: Mathematical Foundations and Applications: West Sussex, UK, Wiley Publishing, 366 p.

Filipponi, M., Jeannin, P.Y., and Tacher, L., 2009, Evidence of inception horizons in karst conduit networks: Geomorphology, v. 106, p. 86–99, doi:10.1016/j.geomorph.2008.09.010.

Florea, L.J., and Wicks, C.M., 2001, Solute transport through laboratory-scale karstic aquifers: Journal of Caves and Karst Studies, v. 63, p. 59–66.

Gilbert, L.E., 1989, Are topographic data sets fractal?: Pure and Applied Geophysics, v. 131, p. 241–254, doi:10.1007/BF00874489.

Grassberger, P., 1981, On the Hausdorff dimension of fractal attractors: Journal of Statistical Physics, v. 26, no. 1, p. 173–179, doi:10.1007/BF01106792.

Jeannin, P.-Y., Groves, C., and Häuselaman, P., 2007, Speleological investigations, *in* Goldscheider, N., and Drew, D., eds., Methods in Karst Hydrogeology: London, UK, Taylor & Francis, p. 25–44.

Kambesis, P.N., 2014, Influence of Coastal Processes on Speleogenesis and Landforms in the Caribbean Region [Ph.D. thesis]: Mississippi State, Mississippi State University, 237 p.

Karperien, A., 1999–2013, FracLac for ImageJ: http://rsb.info.nih.gov/ij/plugins/fraclac/FLHelp/Introduction.htm.

Klinkenberg, B., 1992, Fractals as morphometric measures: Is there a relationship?: Geomorphology, v. 5, p. 5–20, doi:10.1016/0169-555X(92)90055-S.

Labourdette, R., Lascu, I., Mylroie, J.E., and Roth, M., 2007, Process-like modeling of flank-margin caves: From genesis to burial evolution: Journal of Sedimentary Research, v. 77, p. 965–979, doi:10.2110/jsr.2007.086.

Lace, M.J., 2008, Coastal cave development in Puerto Rico: Journal of Coastal Research, v. 24, no. 2, p. 508–518, doi:10.2112/07-0911.1.

Laverty, M., 1987, Fractals in karst: Earth Surface Processes and Landforms, v. 12, p. 475–480, doi:10.1002/esp.3290120505.

Mandelbrot, B., 1983, The Fractal Geometry of Nature: New York, W.H. Freeman, 468 p.

Melo, R.H.C., 2007, Using Fractal Characteristics Such as Fractal Dimension, Lacunarity and Succolarity to Characterize Texture Patterns on Images [Master's thesis]: Niterói, Brazil, Federal Fluminense University, www2.ic.uff.br/PosGraduacao/Dissertacoes/356.pdf.

Mixon, B., 2011, Comment on "Coastal caves in Bahamian aeolian calcarenites: Differentiating between sea caves and flank margin caves using quantitative morphology": Journal of Caves and Karst Studies, v. 73, no. 3, p. 202, doi:10.4311/jcks2011es0195.

Mylroie, J.E., and Carew, J.L., 1990, The flank margin model for dissolution cave formation in carbonate platforms: Earth Surface Processes and Landforms, v. 15, p. 413–424, doi:10.1002/esp.3290150505.

Mylroie, J.R., and Mylroie, J.E., 2007, Development of the carbonate island karst model: Journal of Caves and Karst Studies, v. 69, no. 1, p. 59–75.

Mylroie, J.E., Mylroie, J.R., and Campbell, C.S., 2008, Flank margin cave development in telogenetic limestones of New Zealand: Acta Carsologica, v. 37, no. 1, p. 15–40.

Otoničar, B., Buzjak, N., Mylroie, J.E., and Mylroie, J.R., 2010, Flank margin cave development in carbonate talus breccia facies: An example from Cres Island, Croatia: Acta Carsologica, v. 39, no. 1, p. 79–91.

Owen, A.M., 2007, Tafoni Caves in Quaternary Carbonate Eolianites: Examples from the Bahamas [M.S. thesis]: Mississippi State, Mississippi State University, 187 p.

Owen, A.M., 2013, Tafoni development in the Bahamas, *in* Lace, M.J., and Mylroie, J.E., eds., Coastal Karst Landforms: Heidelberg, Germany, Springer, p. 177–205.

Palmer, A.N., 1991, Origin and morphology of limestone caves: Geological Society of America Bulletin, v. 103, p. 1–21, doi:10.1130/0016-7606(1991)103<0001:OAMOLC>2.3.CO;2.

Palmer, A.N., 2007, Cave Geology: Dayton, Ohio, Cave Books, 454 p.

Palmer, A.N., 2011, Distinction between epigene and hypogene maze caves: Geomorphology, v. 134, p. 9–22, doi:10.1016/j.geomorph.2011.03.014.

Pardo-Igúzquiza, E., Duran-Valsero, J.D., and Rodriguez-Galiano, V., 2011, Morphometric analysis of three-dimensional networks of karst conduits: Geomorphology, v. 132, p. 17–28, doi:10.1016/j.geomorph.2011.04.030.

Pardo-Igúzquiza, E., Dowd, P.A., Xu, C., and Duran-Valsero, J.D., 2012, Stochastic simulation of karst conduit networks: Advances in Water Resources, v. 35, p. 141–150, doi:10.1016/j.advwatres.2011.09.014.

Plotnick, R.E., Gardner, R.H., Hargrove, W.W., Prestegaard, K., and Perlmutter, M., 1996, Lacunarity analysis: A general technique for the analysis of spatial patterns: Physical Review E: Statistical Physics, Plasmas, Fluids, and Related Interdisciplinary Topics, v. 53, no. 5, p. 5461–5468, doi:10.1103/PhysRevE.53.5461.

Rauch, E., 2007, Introduction to lacunarity: www.swiss.ai.mit.edu/~rauch/lacunarity/lacunarity.html (accessed August 2014).

Roth, M.J., 2004, Inventory and Geometric Analysis of Flank Margin Caves of the Bahamas [M.S. thesis]: Mississippi State, Mississippi State University, 117 p.

Shaffer, J.P., 2007, Controlling the false discovery rate with constraints: The Newman-Keuls test revisited: Biometrical Journal (Biometrische Zeitschrift), v. 49, p. 136–143, doi:10.1002/bimj.200610297.

Stafford, K.W., Mylroie, J.E., Mylroie, J.R., Jenson, J.W., and Taborosi, D., 2006, Dissolution controls related to the carbonate island karst model on tectonically active carbonate islands: Tinian and Aguijan, Commonwealth of the Northern Mariana Islands, *in* Davis, R.L., and Gamble, D., eds., Proceedings of the 12th Symposium on the Geology of the Bahamas and Other Carbonate Regions: Concord, New Hampshire, Wallace Press, p. 205–218.

Waterstrat, W.J., Mylroie, J.E., Owen, A.M., and Mylroie, J.R., 2010, Coastal caves in Bahamian aeolian calcarenites: Differentiating between sea caves and flank margin caves using quantitative morphology: Journal of Caves and Karst Studies, v. 72, p. 61–74, doi:10.4311/jcks2009es0086.

Waterstrat, W.J., Mylroie, J.E., Owen, A.M., and Mylroie, J.R., 2011, Reply to comments on: "Coastal caves in Bahamian aeolian calcarenites: Differentiating between sea caves and flank margin caves using quantitative morphology": Journal of Caves and Karst Studies, v. 73, no. 3, p. 203, doi:10.4311/2011ES0216.

Weisstein, E.W., 2006, Mathworld: The Web's Most Extensive Mathematics Resource: http://mathworld.wolfram.com/ (accessed August 2014).

Manuscript Accepted by the Society 17 April 2015
Manuscript Published Online 24 November 2015

Printed in the USA